POLITECNICO DI TORINO
Repository ISTITUZIONALE

Preliminary Assessment of Two Simultaneous and Proportional Myocontrol Methods for 3-DoFs Prostheses Using Incremental Learning

Original
Preliminary Assessment of Two Simultaneous and Proportional Myocontrol Methods for 3-DoFs Prostheses Using Incremental Learning / Egle, F., Di Domenico, D., Marinelli, A., Boccardo, N., Canepa, M., Laffranchi, M., De Michieli, L., Castellini, C.. - ELETTRONICO. - (2023). (IEEE International Conference on Rehabilitation Robotics (ICORR) Singapore, Singapore 24-28 September 2023) [10.1109/ICORR58425.2023.10304813].

Availability:
This version is available at: 11583/2984263 since: 2023-12-07T08:09:59Z

Publisher:
IEEE

Published
DOI:10.1109/ICORR58425.2023.10304813

Terms of use:

This article is made available under terms and conditions as specified in the corresponding bibliographic description in the repository

Publisher copyright
IEEE postprint/Author's Accepted Manuscript

©2023 IEEE. Personal use of this material is permitted. Permission from IEEE must be obtained for all other uses, in any current or future media, including reprinting/republishing this material for advertising or promotional purposes, creating new collecting works, for resale or lists, or reuse of any copyrighted component of this work in other works.

(Article begins on next page)

16 November 2026

Preliminary Assessment of Two Simultaneous and Proportional Myocontrol Methods for 3-DoFs Prostheses using Incremental Learning

Fabio Egle[*,1,†,‡], Dario Di Domenico[*,2,3,‡], Andrea Marinelli[2,4,‡], Nicolò Boccardo[2,5], Michele Canepa[2,5], Matteo Laffranchi[2], Lorenzo De Michieli[2], Claudio Castellini[1,6,‡]

***Abstract*— Despite progressive developments over the last decades, current upper limb prostheses still lack a suitable control able to fully restore the functionalities of the lost arm. Traditional control approaches for prostheses fail when simultaneously actuating multiple Degrees of Freedom (DoFs), thus limiting their usability in daily-life scenarios. Machine learning, on the one hand, offers a solution to this issue through a promising approach for decoding user intentions but fails when input signals change. Incremental learning, on the other hand, reduces sources of error by quickly updating the model on new data rather than training the control model from scratch. In this study, we present an initial evaluation of a position and a velocity control strategy for simultaneous and proportional control over 3-DoFs based on incremental learning. The proposed controls are tested using a virtual Hannes prosthesis on two healthy participants. The performances are evaluated over eight sessions by performing the Target Achievement Control test and administering SUS and NASA-TLX questionnaires. Overall, this preliminary study demonstrates that both control strategies are promising approaches for prosthetic control, offering the potential to improve the usability of prostheses for individuals with limb loss. Further research extended to a wider population of both healthy subjects and amputees will be essential to thoroughly assess these control paradigms.**

I. INTRODUCTION

The loss of a body part significantly affects the quality of life, thus causing physical and psychological consequences. Despite the progressive developments that upper limb prostheses have undergone in the last decades, the rejection rate of such devices is still drastically high ($\sim 44\%$) [1]. One of the main issues related to this low acceptance is the low intuitiveness of the prosthetic control when multiple Degrees of Freedom (DoFs) have to be managed simultaneously [2]. These actuated prostheses are usually controlled through surface electromyographic (sEMG) signals directly gathered from the skin surface. Therefore, the application of machine learning (ML) techniques on sEMG for gesture classification played an important role in the intuitiveness of prosthesis control but with the lack of proportional and simultaneous actuation over multiple DoFs [3]. The regression-based approaches can overcome the aforementioned limits by mapping the predictions in a combination of prosthesis movements [4]. The variability of sEMG signals over time (due to e.g., electrode shift, muscle fatigue, variation in muscle contraction) is the key aspect influencing the deterioration of the prosthesis control [5]. These control paradigms based on supervised ML are characterized by a first phase of training which usually takes a long time [5]. Therefore, if the users realize that the control system no longer works properly, they are forced to retrain from scratch by acquiring a new set of sEMG signals.

To overcome this limitation, we propose two different control paradigms (namely, *direct* and *stepwise* control) based on the same incremental learning algorithm allowing to quickly update the model on a small amount of new data. Moreover, these updates cope with the changes in the input signals, thus allowing continual adaptation of the regression model to the new data distribution [4]. The presented joint control strategies are intended to simultaneously and proportionally control a 3-DoFs Hannes prosthesis [6]. Position and velocity controls have already been used in several previous prosthetic applications ([4, 7, 8, 9]).

In this pilot study, we present the developed system as well as the results of two participants controlling a virtual 3-DoFs Hannes prosthesis in real-time with two different control paradigms (position-based, i.e. *direct control* and velocity-based, i.e. *stepwise control*) based on incremental learning. The interaction with the virtual prosthesis is evaluated over eight sessions per participant by performing the Target Achievement Control (TAC) test [10].

II. MATERIALS AND METHODS

A. Subjects

Two healthy subjects (age: 29 y and 26 y, weight: 70 kg and 86 kg, gender: F and M) with no prior experience in prosthesis control participated in the pilot study. As this is a

This work was partially supported by the European Commission's Horizon Europe Framework Program with the project IntelliMan (AI-Powered Manipulation System for Advanced Robotic Service, Manufacturing and Prosthetics) under Grant Agreement 101070136.

This work was partially supported by INAIL (Istituto Nazionale per l'Assicurazione contro gli Infortuni sul Lavoro) under Grant Agreement: PR19-PAS-P1 - iHannes.

The Open University Affiliated Research Centre at Istituto Italiano di Tecnologia (ARC@IIT) is part of the Open University, Milton Keynes MK7 6AA, United Kingdom.

*These authors equally contributed to this work

†Correspondig author: fabio.egle@fau.de

‡Member IEEE

[1]Assistive Intelligent Robotics Lab, Department Artificial Intelligence in Biomedical Engineering, Friedrich-Alexander-Universität Erlangen-Nürnberg, Erlangen, Germany

[2]Rehab Technologies Lab, Italian Institute of Technology, Via Morego, 30, Genova 16163, Italy

[3]Department of Electronics and Telecommunications, Politecnico di Torino, Turin 10124, Italy

[4]Bioengineering Lab, University of Genova, DIBRIS, Genova, Italy

[5]Open University Affiliated Research Centre at Istituto Italiano di Tecnologia (ARC@IIT), Genova, Italy

[6]Institute of Robotics and Mechatronics, German Aerospace Center, 82234 Wessling, Germany

case study with two subjects, no statistically supported statements are provided. The participants gave written informed consent before the experiments were conducted in line with the Declaration of Helsinki and approved by the institutional ethical committee of Friedrich-Alexander Universität (No.: 22-275-S).

B. Experimental Setup

Two Myos, developed by Thalmic Labs [11] (sampling frequency: 200 Hz, channels: 8, resolution: 8 bit) were attached to the participant's forearm (as depicted in Fig. 1). Both sEMG-devices stream to the same host PC via Bluetooth Low Energy (BLE). The combined 16-channels sEMG signals are then directly processed by a *C#*-based signal-processing application (*Signal Processing* in Fig. 1) in the following steps for each of the channels: (i) amplification (factor: 5) and rectification; (ii) Butterworth lowpass filter [12] (2^{nd} order, direct control: 0.3 Hz, stepwise control: 2 Hz); (iii) subsampling at 25 Hz. After processing, the signals are fed into a Ridge Regression (RR) method, which was previously trained on the subject's signals in an initial training phase (II-E). The RR predictions are clipped to a range from 0 to 1 for each DoF of the respective control (II-D).

The process depicted in Fig. 1 includes three main steps, i.e., the aforementioned sEMG *signals processing*, the *incremental learning* predictions (II-C), and the translation into control signal based on the two different *control strategies* (described in II-D). Once the control signal is synthesized, it is forwarded to the non-immersive Virtual Reality (VR) model. The VR framework itself was implemented using the Unity development framework. The VR model embeds the TAC test (see Fig. 1) used to assess the performance of the used prosthesis control strategy [10]. Three different DoFs could be actively and simultaneously controlled in the Hannes prosthesis [8], namely hand opening/closing (HOC), wrist pronation/supination (WPS) and wrist flexion/extension (WFE). Once the experimenter started the task, the user had 20 s to reach the goal and had to maintain the target configuration for at least 2 s. These time thresholds were already used in other studies, including a TAC test for prosthesis control [10, 13]. The target can assume different configurations of DoFs, combining four positions for the HOC, five positions for WFE, and seven positions for WPS, according to the extent of their range of motion. Additionally, the target position is centered on a tolerance range specific to each joint and control strategy. The thresholds were set to: $th_{HOC} = 0.1$, $th_{WPS} = 0.125$ and $th_{WFE} = 0.083$ for the *stepwise control* strategy while for the *direct control* the thresholds are multiplied by an enlarging factor of 1.5. During each trial, multiple data were collected, and the logging process ran at a mean frequency of 335 Hz. The following parameters were logged: the 16-channels *sEMG* from the two Myos, the *target positions*, which are the goal configurations to reach, the *target errors*, representing the differences in percentage between the current and the target positions over time (separately for each DoF).

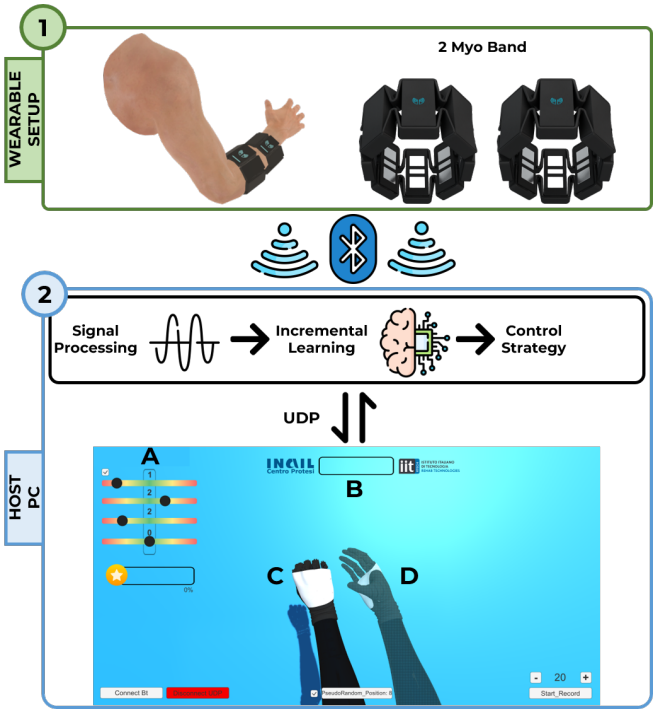


Fig. 1. Block diagram of the experimental setup. *Panel 1*: Wearable setup for EMG acquisition on the forearm consisting of two Myos, which communicate with the host PC via BLE. *Panel 2*: The host PC runs two processes that communicate with each other via User Datagram Protocol (UDP), one dedicated to the processing and inference while the other runs the VR application, including the TAC test. The VR screen shows the sliders representing the current position of each DoF (2.A), the success bar filled up in case all DoFs are in the respective tolerance ranges for 2 s consecutively (2.B), the controlled Hannes prosthesis (2.C) and the target configuration to reach (2.D).

C. Incremental Ridge Regression

To predict the action of each DoF necessary for the respective control paradigm in real-time, the processed sEMG-signals were fed into a RR method [14]. The prediction output is $y = W^T x$, where $x \in \mathbb{R}^{16}$ is the processed sEMG signal and $W \in \mathbb{R}^{16\times d}$ are the regression weights and d is the number of predictions necessary for the respective control paradigm. The closed-form solution for the weights W is given by:

$$W = \left(X^T X + \lambda I\right)^{-1} X^T Y = A^{-1}\beta. \tag{1}$$

The design matrix $X \in \mathbb{R}^{N\times 16}$ consists of the processed 16-channels sEMG signals with N samples. The label matrix $Y \in \mathbb{R}^{N\times C}$ includes the corresponding labels for each DoF of each processed sEMG sample, and the regularization term λ is set to $\lambda = 1$. This value was already used in comparable studies on (virtual) prosthesis control [4, 9]. Instead of completely retraining the predictor after each update by the participant, an incremental approach described by Gijsberts et al. [4] was employed. In brief, the solution in Equation 1 can be decomposed into a product of the inverse matrix A^{-1} and a vector β. With the help of the Sherman–Morrison formula, the update of W by a single added observation x and a label y can be calculated. The RR and the incremental learning

approach were already used in multiple studies in the area of upper limb prosthesis control [4, 15].

D. Control Strategies

In this pilot study, we compare two different control paradigms based on RR, namely the *direct control* and the *stepwise control*. The prediction y of the RR algorithm is exploited by both algorithms but it is treated in different ways. The low-level firmware embedded in the prosthesis is based on position control architecture. However, the synthesis of the control input is different for the two tested paradigms. To distinguish the two controls from the low-level control, the paradigms are denoted as *direct* and *stepwise control* in the following, despite their similarity to position and velocity control, respectively. Each of the two paradigms is a clear representation of two crucial aspects of simultaneous prosthetic control: naturalness and dexterity, respectively. Both characteristics promote man-machine interaction, thus favoring the acceptance of the device.

The *direct control* can be considered as a regressor since the predictions of the RR are directly mapped to a position in the range of motion of each joint. This paradigm resembles position control since the RR prediction outputs are synthesized into reference positions for each DoF. As soon as the subject relaxed the forearm muscles, the prosthesis returned to the resting position. Therefore, the subjects needed to keep the muscle contraction in order to keep the prosthesis in the desired configuration. This resembles what people usually do when they want to move their healthy limbs to manipulate objects. If we want to grasp and lift an object, we are required to maintain muscle contraction, preventing the item from falling. In this case, $d = 5$ control actions were trained, i.e., hand closing (C), wrist pronation (P), wrist flexion (F), wrist extension (E) and resting (R). The opposite movements (i.e., hand opening and wrist supination) were ensured by forearm muscle relaxation. Initial pilot tests during development showed that resting (R) could be used intuitively for hand opening (O) and wrist supination (S).

Before the calculation of the normalized values for the direct prosthesis control, the predictions for each DoF y_i are clipped to a range from 0 to 1 to obtain the corrected predictions $\hat{y}_i$. The normalized control values for HOC ($\theta_{HOC,n}$), WFE ($\theta_{WFE,n}$), and WPS ($\theta_{WPS,n}$) are calculated as:

$$\begin{aligned} \theta_{HOC,n} &= \hat{y}_{C,n}, \\ \theta_{WFE,n} &= \frac{\hat{y}_{E,n} - \hat{y}_{F,n} + 1}{2}, \\ \theta_{WPS,n} &= 1 - \hat{y}_{P,n} \end{aligned} \tag{2}$$

The *stepwise control* is also based on the predictions of the RR algorithm but is mapped to a step-value specific for each DoF. Such a step is added/subtracted to the current position of the respective DoF, thus allowing the subjects to maintain the prosthesis configuration even when there is no muscle contraction. This paradigm resembles velocity control, although the low-level motor actuation is always in position. Therefore, this control paradigm allows holding certain grips even though the user is not performing such movement. In this case, $d = 7$ control actions were trained, i.e., hand closing (C), hand opening (O), wrist pronation (P), wrist supination (S), wrist flexion (F), wrist extension (E), and resting (R). Thus both movements for each of the three DoFs were taken into account. Overall, the resting state corresponds to a fixed configuration of all DoFs. Therefore, once a target position was reached, the subjects could relax their forearm muscles to maintain the target configuration.

Before the calculation of the normalized values for the stepwise prosthesis control, the dead band $d_b = 0.3$ is deducted from the predictions y_i which are then rescaled to the range 0-1 to obtain the corrected prediction $\hat{y}_i$. The normalized control values for HOC, WFE, and WPS ($\theta_{DoF,n}$) are calculated as:

$$\theta_{DoF,n} = \begin{cases} \theta_{DoF,n-1} + d_s \cdot (\hat{y}_{k,n} - \hat{y}_{j,n}) & \text{if } (y_{k,n} \geq d_b \wedge y_{j,n} \geq d_b) \\ \theta_{DoF,n-1}, & \text{otherwise} \end{cases} \tag{3}$$

where k respectively represents C, S, E, and j respectively represents O, P, F, and with the scaling factor $d_s = 4$. The scaling factor is set to the aforementioned value to have the prosthesis in VR moving with a speed comparable to the real Hannes hand.

E. Experimental Protocol

The experiment included eight sessions on four different days, of which four consecutive sessions were dedicated to the *direct control* and the other four to the *stepwise control* (2 sessions/day). Moreover, the order of controls was randomized across the two subjects. This separation between days was intended to test the two conditions over time. The duration of each session was approximately 45 min. Furthermore, each session (S_x) included three consecutive rounds (R_x) and each round in turn 21 target positions (504 target positions per participant). A new RR model was trained at the first use of each control strategy (S_1 and S_5). During this initial training step, the subject performed 3 s of each control action. Before each round, the participants had 2 min to familiarize themselves with the control model by testing it freely. Then, the subject could decide whether to update the model once (twice in S_1 R_1 of each control) by adding additional 3 s of data for each control action (see II-D). Afterward, the learning model was incrementally updated on these labeled data points (15 s for *direct control* or 21 s for *stepwise control*) before starting the next round of the experiment. The model could only be updated at the beginning of a round after the familiarization phase. During the study, the subject sat comfortably in front of a monitor, with their arm slightly flexed and their elbow resting on the table. The computer monitor was placed approximately 50 cm from the subject displaying the VR model. Within each round, the subject was asked to control the Hannes hand in VR to reach the target configuration for 21 runs. The subjects were asked to accomplish the task within 20 s or maintain a position as close as possible to the target. The single run was considered passed in case the subject was able to keep all the controlled DoFs within the established tolerance ranges

(see II-B) for at least 2 s in a row. If the user went out of the tolerance ranges even with any DoF, the 2 s-timer was reset.

At the end of every session, the participant was asked to fill in two questionnaires according to the respective instructions: the NASA Task Load Index (NASA-TLX) parts 1 and 2 [16] was administered to measure perceived cognitive workload during the interaction with the virtual prosthesis as well as the System Usability Score [17] to evaluate the usability of the respective prosthetic control in the context of the given task.

F. Data Analysis

Starting from the retrieved parameters (II-B) logged during the experiments, four different scores are computed to assess the performance of the two control paradigms:

1) *Error Rate*: computed for each DoF as the difference in percentage between the target position and the last reached position in both success and failure runs (i.e., last value of the *target errors* per run);
2) *Success Rate*: the run was counted as a success when the user was able to keep the prosthesis in the target interval of each DoF for 2 s simultaneously;
3) *Path Efficiency*: computed for each DoF as the ratio between the optimal trajectory (an uninterrupted movement toward the target position) and the performed trajectory:

$$\begin{aligned} trj_{act} &= \sum_{i=1}^{N} |\Delta x_i|, \\ trj_{opt} &= x_{tar} - x_0. \end{aligned} \tag{4}$$

   where trj_{act} is the performed trajectory, trj_{opt} is the optimal trajectory, x_i corresponds to a sample of the normalized position, x_{tar} is the target position and N are the samples of each trial;
4) *Time Efficiency*: computed as the ratio between the optimal time needed to reach the target position by the prosthesis in an uninterrupted motion and the time taken by the subject to perform the task.

The questionnaires SUS and NASA-TLX were administered after each session to monitor usability and workload scores over time. The SUS score indicates the usability performance on a scale from 0-100. The questionnaire consists of 10 questions that evaluate the System's usability on a Likert scale from 1 to 5. For the calculation of the score, the reverse-coded questions are negated, and all questions are shifted to a range from 0 to 4. Afterward, the score of the questions is summed and multiplied by 2.5. *Part 1* of the NASA-TLX is a 6-item questionnaire (Mental Demands, Physical Demands, Temporal Demands, Performance, Effort and Frustration) on a scale from *low* to *high*. In *Part 2* of the NASA-TLX the participant decides in a pairwise comparison which factors contributed stronger to the workload. The results of *Part 1* are then weighted by the factors from *Part 2* and averaged to calculate the overall NASA-TLX workload score. In contrast to the original *Part 1* of the NASA-TLX, a visual analog scale was used to describe the workload of each factor continuously.

III. RESULTS

A. TAC

Due to the number of subjects involved in the study, the results are all reported separately for the two participants (p_1 and p_2). As mentioned in II-F, four metrics were computed from the logged data during the TAC test. The aim was to assess the performance of two prosthesis control paradigms based on an incremental learning method. The analysis was performed on different sessions in order to evaluate the learning curve of the subject when controlling the prosthesis. To include the general success information (all DoFs within tolerance ranges), we report the *success rate* computed only in case of complete success of the task. The p_1 scored for *direct control*: S_1 44.4±15.3 - S_4 93.7±2.7, whereas for the *stepwise control*: S_1 58.7±26.2 - S_4 87.3±11.0. The p_2 scored for *direct control*: S_1 30.2±2.7 - S_4 47.6.7±12.6, whereas for the *stepwise control*: S_1 36.5±24.0 - S_4 95.2±4.8. Furthermore, the results are reported independently for each DoF except for the *Time Efficiency* since it is computed on the maximum time of all the controlled joints as they must fall within the tolerance ranges II-B to consider the task accomplished. For all calculated scores, the mean was firstly computed over each round, and then the mean and standard deviation were computed over the three scores of each session (i.e., 3 rounds).

The *Error Rate* is represented separately for each of the two subjects in Fig. 2. Moreover, for each subject, a table (Tab. I) containing the *Success Rate*, the *Path Efficiency* and the *Time Efficiency* is presented. Additionally, for the first two, details regarding the behaviors of each DoF over the sessions are reported. Overall, the two control paradigms are denoted by D (i.e., *direct control*) and S (i.e., *stepwise control*).

B. Questionnaires

For the participants in this pilot study, the given answers to the questionnaires were fairly positive. Particularly interesting was the development of the scores over the 4 sessions (12 rounds of 21 tasks). The individual scores per session and participant are presented in Tab. II and Tab. III. The SUS score can range from 0 to 100, with a higher score meaning better usability. The mean SUS scores over the four sessions per participant and algorithm were 79.38±7.18 (p_1) and 55.63±8.75 (p_2) for the *direct control* as well as 68.75±14.79 (p_1) and 75.00±4.56 (p_2) for the *stepwise control*. The SUS scores over sessions are reported in Tab. II, where the S_4 achieved the highest ratings for both controls and participants.

The NASA-TLX outcomes for the 2 participants were similarly positive. Same as the SUS, the NASA-TLX can also range from 0 to 100, although, in this case, a lower score indicates a lower workload. The mean scores over the four sessions for the *direct control* were 37.87±9.16 (p_1) and 58.64±15.20 (p_2). The results for the *stepwise control* were 57.00±11.22 (p_1) and 30.09±5.53 (p_2). Similar to the usability evaluation, the workload score generally indicates

TABLE I

SCORES OF p_1 AND p_2 FROM TAC TEST

	Parameter	*Control*	S_1			S_2			S_3			S_4		
			HOC	*WPS*	*WFE*	*HOC*	*WPS*	*WFE*	*HOC*	*WPS*	*WFE*	*HOC*	*WPS*	*WFE*
p_1	*Success Rate*	D	60.3±12.0	54.0±15.3	55.6±11.0	82.5±2.7	73.0±11.0	79.4±2.7	95.2±8.2	90.5±8.2	95.2±8.2	96.8±2.7	93.7±2.7	93.7±2.7
		S	71.4±21.8	63.5±27.1	82.5±30.2	85.7±4.8	77.8±5.5	96.8±2.7	96.8±2.7	92.1±9.9	93.7±2.7	90.5±8.2	92.1±7.3	96.8±5.5
	Path Efficiency	D	15.3±8.3	23.6±6.3	11.1±9.9	23.9±6.5	24.2±6.0	20.2±3.0	25.3±1.5	26.7±1.3	22.0±3.8	28.4±3.0	23.5±2.3	18.6±4.3
		S	28.9±9.4	23.0±2.1	38.8±17.9	42.0±2.3	31.0±5.2	48.3±2.3	39.3±4.5	27.9±2.6	51.9±10.6	40.8±2.0	31.5±2.1	52.6±4.8
	Time Efficiency	D		20.5±3.7			25.9±4.6			29.6±2.0			28.0±3.1	
		S		12.5±1.3			15.9±1.8			14.7±2.5			14.8±0.4	
p_2	*Success Rate*	D	44.4±12.0	44.4±5.5	46.0±7.3	39.7±7.3	52.4±9.5	46.0±2.7	57.1±4.8	61.9±4.8	69.8±7.3	54.0±14.5	60.3±11.0	71.4±9.5
		S	47.6±26.5	65.1±22.5	44.4±19.2	79.4±15.3	90.5±4.8	85.7±8.2	96.8± 5.5	98.4± 2.7	96.8±5.5	95.2±4.8	98.4± 2.7	95.2±4.8
	Path Efficiency	D	19.7±6.2	11.6±7.9	11.4±1.7	15.0±1.3	11.7±6.0	10.8±2.7	17.7±3.7	13.1±2.8	9.0±1.9	14.9±2.3	15.3±2.2	5.4±0.7
		S	38.6±18.4	39.6±15.7	24.9±7.5	29.9±6.5	38.4±3.1	26.6±3.4	28.2±4.5	46.6±4.6	27.6±3.0	21.7±8.9	43.2±9.0	24.1±4.2
	Time Efficiency	D		18.6±2.6			20.8±6.2			20.5±2.4			21.6±4.2	
		S		14.9±1.9			18.8±3.1			23.8±2.6			20.7±2.4	

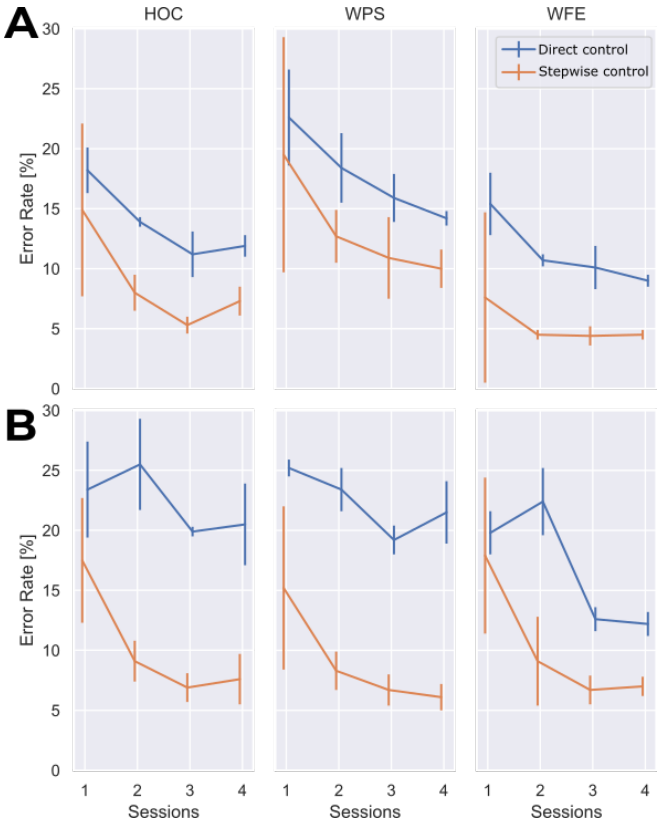


Fig. 2. **A**: Error Rate as a function of the Sessions for p_1 in the two tested control modalities. **B**: Error Rate as a function of the Sessions for p_2 in the two tested control modalities. The mean and standard deviation of the Error Rate are computed on the percentage of successful runs within each round. The vertical bars represent a standard deviation. A representation for each DoF (i.e., HOC: hand opening/closing, WPS: wrist pronation/supination, WFE: wrist flexion/extension) is reported in both panels (A, B).

a decrease in workload with the time spent controlling the virtual prosthesis (see Tab. III).

IV. DISCUSSION AND CONCLUSION

Starting from the results depicted in Fig. 2, for both the two control strategies, the *Error Rate* showed decreasing trend when comparing the first and the last session. Moreover, the standard deviation has a similar behavior, thus supporting the hypothesis that a higher training involvement

TABLE II

SCORES OF THE SYSTEM USABILITY SCALE (SUS)

Participant	***Control***	S_1	S_2	S_3	S_4
p_1	D	70.00	77.50	85.00	85.00
	S	55.00	57.50	77.50	85.00
p_2	D	45.00	52.50	60.00	65.00
	S	72.50	70.00	77.50	80.00

TABLE III

SCORES OF THE NASA - TASK LOAD INDEX (NASA-TLX)

Participant	***Control***	S_1	S_2	S_3	S_4
p_1	D	45.01	45.84	26.90	33.75
	S	63.20	68.57	52.99	43.24
p_2	D	68.96	73.94	49.27	42.37
	S	35.43	33.77	23.46	27.71

of the participant results in a finer control for the proposed systems. In addition, the overall *Success Rate* confirms the learning process over sessions for both participants. For the two control strategies, the mean of the *Success Rate* in S_4 outperforms S_1. The reduction of the standard deviations computed on *Success Rate* over sessions demonstrates improvement in prosthesis control skills. Concerning the *Path Efficiency*, it has a similar trend to the aforementioned scores when considering the first and last sessions for both the control strategies. It underlines the training of the participants and their increasing ability to take shorter routes in the joint space when reaching the target positions. The results are reported separately for each DoF to highlight, if present, the ability to control one joint better than the others. As for the *Time Efficiency*, it increased over the sessions meaning that the participants were able to accomplish the task in a shorter time. Although the *stepwise control* has narrower tolerance ranges than *direct control*, it achieved more promising results. The authors hypothesize that *stepwise control* by design is more reliable when holding grips for a long time since the prosthesis stops in the last reached position in case of muscle

relaxation.

The results of TAC test scores are also reflected in the results of the questionnaires. In S_1 medium scores were given by the naive subjects. For both questionnaires, the SUS and the NASA-TLX, the scores improved considerably from the first to the last session. These results indicate that the usability is estimated to be higher and the workload to be lower over time. This is another indicator of the usefulness of the multi-session setup for the evaluation of prosthesis control. In the future, this pilot study needs to be extended to a larger population to confirm these initial results. Furthermore, with more participants, single factors from the questionnaires can be identified which contribute most to the change in usability and workload, respectively.

The two proposed control paradigms might be crucial in prosthesis applications since they allow to simultaneously control a 3-DoFs prosthesis in real-time. An important aspect of these control paradigms is the short training time since just 3 s of sEMG signal are acquired for each control action. Therefore, the RR model was initially trained on 15s of sEMG ($d = 5$) for *direct control* and 21s of sEMG ($d = 7$) for the *stepwise control*. Additionally, the use of 16 sEMG channels (2 Myos) was suitable to simultaneously and proportionally control the 3-DoFs Hannes system [9]. However, this setup has some limitations in the application to amputees due to its dimensions. Therefore, we are currently running experiments on prosthesis users exploiting fewer sEMG electrodes with smaller shapes. Moreover, it may be worth studying the role of higher resolution or number of sEMG sensors on prediction accuracy by exploiting smaller electrodes.

In future applications, both control strategies might be embedded in the prosthetic device allowing the user to switch between algorithms depending on their needs. The results of this pilot study suggest that *direct control* could be more natural and intuitive. This could be due to the replication of the natural encoding scheme of the hand [7, 18]. In contrast, the *stepwise control* could be more dexterous and robust thanks to its stability in the movements. Overall, these encouraging results must be confirmed on a larger population of healthy subjects and subsequently verified on individuals with amputation, thus assessing such performance for prosthesis users.

REFERENCES

[1] S. Salminger, H. Stino, L. H. Pichler, C. Gstoettner, A. Sturma, J. A. Mayer, M. Szivak, and O. C. Aszmann, "Current rates of prosthetic usage in upper-limb amputees – have innovations had an impact on device acceptance?" *Disability and Rehabilitation*, vol. 44, no. 14, pp. 3708–3713, Jul. 2022. [Online]. Available: https://www.tandfonline.com/doi/full/10.1080/09638288.2020.1866684

[2] T. J. Bates, J. R. Fergason, and S. N. Pierrie, "Technological advances in prosthesis design and rehabilitation following upper extremity limb loss," *Current reviews in musculoskeletal medicine*, vol. 13, pp. 485–493, 2020, publisher: Springer.

[3] A. Marinelli, N. Boccardo, F. Tessari, D. D. Domenico, G. Caserta, M. Canepa, G. Gini, G. Barresi, M. Laffranchi, L. D. Michieli, and M. Semprini, "Active upper limb prostheses: a review on current state and upcoming breakthroughs," *Progress in Biomedical Engineering*, vol. 5, no. 1, p. 012001, Jan. 2023, publisher: IOP Publishing. [Online]. Available: https://dx.doi.org/10.1088/2516-1091/acac57

[4] A. Gijsberts, R. Bohra, D. Sierra González, A. Werner, M. Nowak, B. Caputo, M. Roa, and C. Castellini, "Stable myoelectric control of a hand prosthesis using non-linear incremental learning," *Frontiers in Neurorobotics*, vol. 8, 2014. [Online]. Available: https://www.frontiersin.org/articles/10.3389/fnbot.2014.00008

[5] A. Phinyomark and E. Scheme, "EMG Pattern Recognition in the Era of Big Data and Deep Learning," *Big Data and Cognitive Computing*, vol. 2, no. 3, 2018. [Online]. Available: https://www.mdpi.com/2504-2289/2/3/21

[6] M. Laffranchi, N. Boccardo, S. Traverso, L. Lombardi, M. Canepa, A. Lince, M. Semprini, J. A. Saglia, A. Naceri, and R. Sacchetti, "The Hannes hand prosthesis replicates the key biological properties of the human hand," *Science robotics*, vol. 5, no. 46, p. eabb0467, 2020, publisher: American Association for the Advancement of Science.

[7] J. A. George, D. T. Kluger, T. S. Davis, S. M. Wendelken, E. V. Okorokova, Q. He, C. C. Duncan, D. T. Hutchinson, Z. C. Thumser, D. T. Beckler, P. D. Marasco, S. J. Bensmaia, and G. A. Clark, "Biomimetic sensory feedback through peripheral nerve stimulation improves dexterous use of a bionic hand," *Science Robotics*, vol. 4, no. 32, p. eaax2352, Jul. 2019, publisher: American Association for the Advancement of Science. [Online]. Available: https://www.science.org/doi/10.1126/scirobotics.aax2352

[8] D. Di Domenico, A. Marinelli, N. Boccardo, M. Semprini, L. Lombardi, M. Canepa, S. Stedman, A. D. Bellingegni, M. Chiappalone, and E. Gruppioni, "Hannes prosthesis control based on regression machine learning algorithms." IEEE, 2021, pp. 5997–6002.

[9] M. Nowak, I. Vujaklija, A. Sturma, C. Castellini, and D. Farina, "Simultaneous and Proportional Real-Time Myocontrol of Up to Three Degrees of Freedom of the Wrist and Hand," *IEEE Transactions on Biomedical Engineering*, vol. 70, no. 2, pp. 459–469, Feb. 2023, conference Name: IEEE Transactions on Biomedical Engineering.

[10] A. M. Simon, L. J. Hargrove, B. A. Lock, and T. A. Kuiken, "The target achievement control test: Evaluating real-time myoelectric pattern recognition control of a multifunctional upper-limb prosthesis," *Journal of rehabilitation research and development*, vol. 48, no. 6, p. 619, 2011, publisher: NIH Public Access.

[11] "Thalmic Labs · GitHub." [Online]. Available: https://github.com/thalmiclabs

[12] S. Butterworth, "On the theory of filter amplifiers," *Experimental Wireless*, pp. 536–541, Oct. 1930.

[13] R. B. Woodward and L. J. Hargrove, "Adapting myoelectric control in real-time using a virtual environment," *Journal of neuroengineering and rehabilitation*, vol. 16, no. 1, pp. 1–12, 2019, publisher: BioMed Central.

[14] A. E. Hoerl and R. W. Kennard, "Ridge Regression: Biased Estimation for Nonorthogonal Problems," *Technometrics*, vol. 12, no. 1, pp. 55–67, Feb. 1970. [Online]. Available: 10.1080/00401706.1970.10488634

[15] F. Schiel, A. Hagengruber, J. Vogel, and R. Triebel, "Incremental learning of EMG-based control commands using Gaussian processes." PMLR, 2021, pp. 1137–1146.

[16] S. G. Hart and L. E. Staveland, "Development of NASA-TLX (Task Load Index): Results of Empirical and Theoretical Research," in *Advances in Psychology*, ser. Human Mental Workload, P. A. Hancock and N. Meshkati, Eds. North-Holland, Jan. 1988, vol. 52, pp. 139–183. [Online]. Available: https://www.sciencedirect.com/science/article/pii/S0166411508623869

[17] J. Brooke and others, "SUS-A quick and dirty usability scale," *Usability evaluation in industry*, vol. 189, no. 194, pp. 4–7, 1996, publisher: London–.

[18] J. M. Goodman, G. A. Tabot, A. S. Lee, A. K. Suresh, A. T. Rajan, N. G. Hatsopoulos, and S. Bensmaia, "Postural Representations of the Hand in the Primate Sensorimotor Cortex," *Neuron*, vol. 104, no. 5, pp. 1000–1009.e7, Dec. 2019. [Online]. Available: https://linkinghub.elsevier.com/retrieve/pii/S0896627319307779